Multi-UAV Replacement and Trajectory Design for Coverage Continuity

Nishant Gupta[1], Satyam Agarwal[1], and Deepak Mishra[2]

[1]Department of Electrical Engineering, Indian Institute of Technology Ropar, Punjab, India
[2]School for Electrical Engineering and Telecommunications, University of New South Wales, Sydney, Australia
E-mails: nishantgupta.nic@gmail.com, satyam6099@gmail.com, dph.mishra@gmail.com

ICC 2022 - IEEE International Conference on Communications | 978-1-5386-8347-7/22/$31.00 ©2022 IEEE | DOI: 10.1109/ICC45855.2022.9838297

***Abstract*—In this paper, we present a novel framework to maintain coverage continuity in a unmanned aerial vehicle (UAV)-assisted wireless communication system, when a serving UAV runs out of energy. Service continuity is maintained by launching another fully charged UAV to replace the existing serving UAV. This replacement process must ensure maximal coverage to all ground users. Our objective during this replacement process is to maximize the achievable sum rate of all ground users by jointly optimizing the three-dimensional (3D) multi-UAVs trajectory and resource allocation to the users from the individual UAVs. This is carried out in the presence of the UAV's constraints on velocity, collision avoidance, and energy availability while considering a more practical and accurate probabilistic line-of-sight (LoS) channel model. This results in a non-convex optimization problem for which an efficient iterative algorithm based on successive convex approximation and alternating optimization is proposed. Numerical results are provided to obtain insights on the UAV trajectories and the effectiveness of the proposed scheme compared to the existing benchmark schemes is shown.**

***Index Terms*—Multi-UAV, 3D trajectory, resource allocation, energy availability, UAV replacement**

I. Introduction

Unmanned aerial vehicles (UAVs) have emerged as a new technology to assist wireless communication due to the exponential increase in data traffic. Owing to their advantages, such as fully controllable mobility, ability to hover and maintain line-of-sight (LoS) communication links, UAVs are frequently used as an on-demand base station (BS) to offload the data traffic in certain scenarios like sports events, fairs, carnivals, and specific disaster-related incidents [1]. Despite, the UAVs pose certain challenges, such as three-dimensional (3D) deployment location where a UAV must be deployed to deliver fruitful service to the ground users along with the UAV trajectory to maximize the system's performance. Also, the UAV's limited energy availability inhibits the UAV from delivering long-term service.

Given the limited on-board energy, the UAV must be grounded frequently to replenish their battery. To maintain coverage continuity, the existing serving UAV must be replaced by another fully charged UAV when its available energy is exhausted. As another UAV is launched for replacement, multiple key challenges like user association, resource allocation and 3D multi-UAVs trajectory planning must be addressed in the presence of UAV energy consumption constraints.

Motivated by the UAV replacement scenario and its challenges, this paper present a novel framework for maintaining coverage continuity in a UAV-assisted communication system by launching a fully charged UAV to replace the existing UAV. This is accomplished by optimizing the 3D multi-UAVs trajectory, user association, and resource allocation [2] to maximize the system's achievable sum rate in a more realistic UAV-user probabilistic LoS channel model. Apart from this, we also consider practical UAV constraints, such as UAV mobility, collision avoidance, and energy consumption.

In the existing literature, the authors in [3], maximized the minimum throughput by jointly optimizing the two-dimensional (2D) trajectory and transmit power. Similarly, in [4], the authors jointly optimized the user association, 2D UAV trajectory and power control in a LoS dominant UAV-user channel model. The authors in [5] studied the multi-UAV wireless powered system where multiple UAVs are dispatched as energy transfer source to internet-of-things (IoT) users. It jointly optimized the resource allocation and 2D UAV trajectory. The above works [3]–[5] either considered the 2D UAV trajectory or LoS UAV-user channel model. However, while designing the UAV communication system, a more realistic and practical UAV-user channel model should be considered along with the 3D trajectory.

Towards this end, the 3D multi-UAVs trajectory was optimized in [6]–[9] to maximize the system performance. The works [6], and [7] jointly optimized resource allocation and 3D UAV trajectory but for a LoS dominant UAV-user channel. The authors in [8], and [9], considered a realistic channel model that comprises of both the LoS and non-LoS (NLoS) links *i.e.,* probabilistic LoS model to jointly optimize the 3D UAV trajectories. In particular, [8], maximized the downlink capacity to design the 3D trajectory of multi-UAV system while ignoring the energy availability of the UAV and the optimal power allocated to user. Moreover, [9] considered the wireless power transfer IoT system that jointly optimized the UAV trajectory and time allocated to each user in the presence of UAV's on-board energy constraint. A short summary of existing works on multi-UAV system with their key differences with our work is shown in Table I.

The works [3]–[5], [7], assumed the UAV to return to its initial location at the end of the time period. Furthermore, in [3]-[9], it is assumed that in each time slot, a UAV serves atmost one user. Thus, apart from optimizing the power allocation and the 3D multi-UAVs trajectory in the probabilistic LoS channel model, the replacement process, where the new UAV replaces the existing UAV when each serves multiple users, has not been studied in the literature.

TABLE I: Short summary of related work with their key difference. **C**, **E**, and **P** is the channel, energy, and power, respectively.

Ref.	Optimization variable	C	E	P
[3]	Cache placement, power, 2D trajectory	LoS	×	✓
[4]	User association, power and 2D trajectory	LoS	×	✓
[5]	User association, power, 2D trajectory	LoS	×	✓
[6]	User association, power, 3D trajectory	LoS	×	✓
[7]	3D trajectory and power control	LoS	×	✓
[8]	User association, 3D trajectory	P-LoS	×	×
[9]	Time allocation, 3D trajectory	P-LoS	✓	×
Ours	User association, power, 3D trajectory	P-LoS	✓	✓

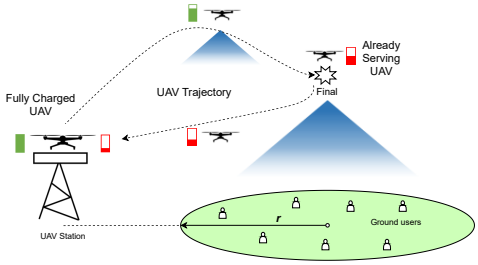

Fig. 1: System model representing the coverage field having N users along with UAV's initial and final locations.

Therefore, this paper studies the novel framework of UAV replacement process in a UAV-assisted communication system.

II. Downlink System Model

A. UAV Trajectory Model

We consider a UAV-assisted communication system with $\mathcal{K} = \{1, \cdots, K\}$ ground users that are distributed over an area. Location of the k^{th}-user is given by $\mathbf{w}_k = [x_k, y_k]$, where $k \in \mathcal{K}$. The users are assumed to be stationary and their location is known. To consider the UAV replacement scenario, we consider $m \in \{1, 2\}$ UAVs. One is the existing UAV, denoted by $U_1(m = 1)$ and the other is a new fully charged UAV, denoted by $U_2(m = 2)$. At the start of the replacement process, we assume that U_1 is located at $\mathbf{X}_F$ and is serving users while U_2 is launched from location $\mathbf{X}_I$ to replace U_1. Over time T, the replacement of the UAV takes place with U_2 taking position $\mathbf{X}_F$ while U_1 returning back to the charging location $\mathbf{X}_I$. Then, the constraint on UAV location is given as

$$\mathbf{X}_1[0] = \mathbf{X}_F, \mathbf{X}_1[N] = \mathbf{X}_I, \mathbf{X}_2[0] = \mathbf{X}_I, \mathbf{X}_2[N] = \mathbf{X}_F, \tag{1}$$

where $\mathbf{X}_I = [x_I, y_I, z_I]$ and $\mathbf{X}_F = [x_F, y_F, z_F]$.

For analytical tractability, we assume the total flight time T of the UAV is discretized into N slots of equal length. The slot duration is given by $\tau = T/N$. The slot duration τ is set to be sufficiently small such that the UAV is assumed to be stationary within the time slot [10]. The UAV location at n^{th}-time slot is given by $\mathbf{X}_m[n] = [\mathbf{q}_m[n], z_m[n]]$, where $m \in \{1, 2\}$. $\mathbf{q}_m[n]$ and $z_m[n]$ are the horizontal and vertical coordinate of the m^{th}-UAV, respectively. Note that, in our work, we consider two-UAVs for better insights but this work is also valid for more than two UAVs.

We assume the maximum flying velocity of the UAV is constrained by V^m_{max} such that $v_m[n] \leq V^m_{max}, \forall n, m \in \{1, 2\}$, where $v_m[n]$ is the velocity of m^{th}-UAV at time slot n. $v_m[n] = d_m[n]/\tau$, where $d_m[n] = \|\mathbf{X}_m[n] - \mathbf{X}_m[n-1]\|$ is the distance travelled by the m^{th}-UAV in the n^{th}-time slot. In this multi-UAV system, for simplicity, we assume the minimum horizontal distance required between the UAVs to avoid collision is D_{min}.

We define a binary variable $a_{k,m}[n]$, which represents the association of the k^{th}-user to the m^{th}-UAV at n^{th}-time slot. If $a_{k,m}[n] = 1$, means the k^{th}-user is connected to the m^{th}-UAV at the n^{th}-time slot, otherwise, $a_{k,m}[n] = 0$. We assume in a particular slot, a user is connected to a single UAV. Thus, we get the following constraints on the user association

$$a_{k,m}[n] \in \{0, 1\}, \forall k, n, m \in \{1, 2\}, \tag{2}$$

$$\sum_{m=1}^{2} a_{k,m}[n] = 1, \forall k, n. \tag{3}$$

Also, let $p_{k,m}$ denotes the power allocated to the k^{th}-user by the m^{th}-UAV at time slot n in a downlink communication. Due to the limited power of UAV, the constraint on the power allocation is given by

$$\sum_{k=1}^{K} a_{k,m}[n] p_{k,m}[n] \leq P_{max}, \forall n, m \in \{1, 2\}, \tag{4}$$

where P_{max} is the maximum power to be allocated from the UAV for providing communication.

In this work, we make use of a rotary-wing UAVs because of its additional hovering feature over the fixed-wing UAV. The energy model of a rotary-wing UAV as a function of velocity is given as [11, Eq. 16]

$$e_m[n] = \tau P_o \left(1 + \frac{3v_m[n]^2}{U^2_{tip}}\right) + \tau P_i \left(\sqrt{1 + \frac{v_m[n]^4}{4v_o^2}} - \frac{v_m[n]^2}{2v_o^2}\right)^{\frac{1}{2}} + \tau \frac{1}{2} d_0 \rho S A v_m[n]^3 + \vartheta v_c, \tag{5}$$

where v_o is the mean rotor induced velocity. U_{tip} is the tip speed of rotor blade. d_0, ρ, and S are the fuselag ratio, air density, and rotor solidity, respectively. A and v_c represent the rotor disc area, and speed of climb, respectively. P_o and P_i are the constants and denote the blade profile power and induced power, respectively. $\vartheta = W + \frac{1}{2}\rho s_{sp} v_m[n]^2 \sin\varphi$, where W is the thrust of UAV, φ is the climb/descent angle and s_{sp} is constant. The overall energy consumption constraint of the m^{th}-UAV is given by

$$\sum_{n=1}^{N} e_m[n] \leq E^m_{max}, \forall m \in \{1, 2\}, \tag{6}$$

where E^m_{max} is the energy available of the m^{th}- UAV.

B. Air-to-Ground (A2G) Channel Model

The A2G channel includes both the LoS and NLoS components depending upon the environment. Therefore, we consider a probabilistic LoS channel model wherein, the LoS and NLoS links have certain occurrence probability. Then, the path loss for LoS and NLoS links are expressed as $L^{k,m}_L[n] = \beta_0 d_{k,m}[n]^{-\bar{\alpha}}$, and $L^{k,m}_N[n] = \kappa\beta_0 d_{k,m}[n]^{-\bar{\alpha}}$, respectively. Here $d_{k,m}[n]$ represents the distance between the k^{th}-user and the m^{th}-UAV, given by

$d_{k,m}[n] = \sqrt{\|\mathbf{q}_m[n] - \mathbf{w}_k\| + z_m[n]^2}$. $\beta_0, \bar{\alpha}$, and κ denote the pathloss at reference distance, pathloss exponent, and additional attenuation factor, respectively.

The probability of LoS link (P^L) depends upon the elevation angle (in degrees) of the m^{th}-UAV with the k^{th}-user given by $\phi_{k,m}[n] = \tan^{-1}\left(\frac{z_m[n]}{\|\mathbf{q}_m[n]-\mathbf{w}_k\|}\right)$. Thus, $P^L_{k,m}[n]$ is given by $P^L_{k,m}[n] = \frac{1}{(1+C\exp(-D[\phi_{k,m}[n]-C]))}$, where C and D are parameters describing the suburban, urban, or dense urban environment.

The average channel gain $h_{k,m}[n]$ between the m^{th}-UAV and the k^{th}-user at time slot n is expressed as

$$\begin{aligned} h_{k,m}[n] =& P^L_{k,m}[n]L^{k,m}_L[n] + (1 - P^L_{k,m}[n])L^{k,m}_N[n] \\ =& \beta_0 \frac{(1-\kappa)P^L_{k,m}[n] + \kappa}{\|\mathbf{q}_m[n] - \mathbf{w}_k\|^2 + z_m[n]^2}. \end{aligned} \tag{7}$$

In this paper, we focus on the frequency division multiple access (FDMA) scheme for sharing resources among ground users. We assume that the UAVs allocate equal bandwidth B and independent channels to all ground users. Then, the signal to noise ratio (SNR) at the k^{th}-user denoted by $\gamma_{k,m}[n]$ is given by $\gamma_{k,m}[n] = \frac{P_{k,m}[n]h_{k,m}[n]}{\sigma^2}$ [12]. Then, the achievable data rate at the k^{th}-user from the m^{th}-UAV at time slot n is given by

$$\mathcal{R}_{k,m}[n] \approx \frac{B}{K} a_{k,m}[n] \log_2\left(1 + \gamma_{k,m}[n]\right). \tag{8}$$

C. Problem Formulation

In this paper, we intent to maximize the achievable sum rate over all users and time in a UAV-assisted communication system. This objective is chosen to target the applications with system-centric goal rather than the user-level. We define $\mathbf{A} = \{a_{k,m}[n], \forall k, m, n\}$, $\mathbf{P} = \{p_{k,m}[n], \forall k, m, n\}$ and $\mathbf{T} = \{\mathbf{X}_m[n], \forall m, n\}$ as user association, user power allocation, and UAV trajectory, respectively. The optimization problem is formulated as

$$\begin{aligned} \mathbf{P1}: \max_{\mathbf{A},\mathbf{P},\mathbf{Q}} \quad & \mathcal{R} \triangleq \sum_{n=1}^{N}\sum_{k=1}^{K}\sum_{m=1}^{2} \mathcal{R}_{k,m}[n], \\ s.t.\ & (1)-(4), (6) \\ & v_m[n] \le V^m_{max}, \forall m, n, && \text{(9a)} \\ & z_m[n] \ge H, \forall m, n, && \text{(9b)} \\ & \|\mathbf{q}_m[n] - \mathbf{q}_j[n]\|^2 \ge D^2_{min}, \forall n, m \ne j, && \text{(9c)} \end{aligned}$$

where (9a) is the maximum velocity constraint, (9b) is the minimum height constraint to ensure safety flight, and (9c) is the collision avoidance constraint. It can be observed that the problem **P1** is highly complex and is difficult to be solved due to the following reasons. First, the user association constraint in (2) is binary, so (3), and (4) contains integer variables. Second, the constraints (6), and (9c) are non-convex constraints. Third, the objective function is non-concave. Therefore, the problem **P1** is a mixed-integer non-convex problem, which cannot be easily solved.

III. Proposed Approach

In this section, we propose a low-complexity alternating optimization (AO) algorithm that successively optimize **A**, **P**, and **T** to maximize the sum rate. To make the problem **P1** tractable, we transform the binary variable $a_{k,m}[n]$ to a continuous variable in constraint (2) in **P1** as

$$0 \le a_{k,m}[n] \le 1, \forall k, m, n. \tag{10}$$

With this relaxed constraint (10) instead of (2) in **P1**, we decouple the relaxed **P1** into three sub-problems. Optimize user association **A**, optimize user power allocation **P**, and optimize multi-UAVs trajectory **T**. These are solved by keeping the variables of other subproblems fixed.

A. User Association

By taking the given power allocation **P** and the multi-UAVs trajectory **T**, the user association subproblem is given as

$$\mathbf{P2}: \quad \max_{\mathbf{A}} \quad \mathcal{R}, \quad s.t. \quad (10), (3), (4).$$

It can be easily observed that the problem **P2** is a standard linear programming and can be solved by using the existing optimization methods. Note that the solution **A** can be made integer by using the rounding method described in [4].

B. Multi-UAVs Trajectory

Here, we optimize the multi-UAVs trajectory for any given **A** and **P**. Then, the trajectory problem is formulated as

$$\mathbf{P3}: \quad \max_{\mathbf{T}} \quad \mathcal{R}, \quad s.t. \quad (1), (9a), (9b), (9c).$$

Note that here we have relaxed the energy constraint (6) because the energy model of UAV is a function of velocity. Therefore, to satisfy the energy, we can iterate the solution by varying the UAV velocity as described in Section III-D. The problem **P3** is a non-convex problem due to the presence of non-concave objective function and the non-convex constraint (9c). To solve this problem, we divide the problem into a sequence of subproblems where we first obtain the UAV locations in each time slot and then constructs the trajectory based on those locations. Then, the problem valid for a single time slot is given by

$$\mathbf{P3.1}: \max_{\mathbf{q}_m[n], z_m[n], \forall m} \sum_{k=1}^{K}\sum_{m=1}^{2} \mathcal{R}_{k,m}[n], \ s.t.\ (9a) - (9c),$$

where $\mathcal{R}_{k,m}[n]$ is given as

$$\mathcal{R}_{k,m}[n] = \frac{B a_{k,m}[n]}{K} \log_2\left(1 + \tilde{\gamma_o} \frac{p_{k,m}[n]((1-\kappa)P^L_{k,m}[n] + \kappa)}{\|\mathbf{q}_m[n] - \mathbf{w}_k\|^2 + z_m[n]^2}\right). \tag{14}$$

The problem **P3.1** is non-convex. Here, we first transform the objective function. To deal with $\mathcal{R}_{k,m}[n]$ in (14), we introduce an auxiliary variable $\alpha_{k,m}[n]$ which can be represented as

$$\alpha_{k,m}[n] \le \frac{(1-\kappa)P^L_{k,m}[n] + \kappa}{\|\mathbf{q}_m[n] - \mathbf{w}_k\|^2 + z_m[n]^2}. \tag{15}$$

For ease of representation of $P^L_{k,m}[n]$, we take $\Phi_{k,m}[n] = \frac{z_m[n]}{\|\mathbf{q}_m[n]-\mathbf{w}_k\|}$ such that $P^L_{k,m}[n]$ can be expressed as

$$P^L_{k,m}[n] = \left(1 + C\exp\left(-D\left[\tan^{-1}\Phi_{k,m}[n] - C\right]\right)\right)^{-1}. \tag{16}$$

Substituting (16) into (15), is still non-convex, therefore we introduce an auxiliary variable $y_{k,m}[n]$ such that $0 \le$

$y_{k,m} \leq P^L_{k,m}[n]$, which can be equivalently represented by

$$1+C\exp\left(-D\left[\tan^{-1}\Phi_{k,m}[n]-C\right]\right)-\frac{1}{y_{k,m}[n]}\leq 0, \quad (17)$$

$$y_{k,m}[n] \geq 0. \quad (18)$$

To make inequality in (15) more tractable, we introduce an auxiliary variable $\beta_{k,m}[n]$ such that

$$\alpha_{k,m}[n](\|\mathbf{q}_m[n]-\mathbf{w}_k\|^2+z_m[n]^2) \leq \beta_{k,m}[n], \text{and} \quad (19)$$

$$(1-\kappa)y_{k,m}[n]+\kappa \geq \beta_{k,m}. \quad (20)$$

Then, the inequality (15) can be equivalently represented by (17)-(20). Thus, problem **P3.1** can be transformed to

$$\textbf{P3.2}: \max_{\mathcal{X}} \sum_{k=1}^{K}\sum_{m=1}^{2}\frac{Ba_{k,m}[n]}{K}\log_2(1+\tilde{\gamma_o}p_{k,m}[n]\alpha_{k,m}[n]),$$

$$s.t.\ (9a)-(9c), (17)-(20) \quad (21a)$$

$$\Phi_{k,m}[n]=\frac{z_m[n]}{\|\mathbf{q}_m[n]-\mathbf{w}_k\|}, \quad (21b)$$

where $\mathcal{X}=\{\mathbf{q}_m[n], z_m[n], \alpha_{k,m}[n], \Phi_{k,m}[n], y_{k,m}[n], \beta_{k,m}[n]\}, \forall m$. In the above problem, the constraints (9c), (17), (19) and (21b) are non-convex. To transform the problem into the convex problem, we next introduce the lemmas to convexify the constraints.

Lemma 1: The constraint (21b) can be represented in the convex form which is given by

$$\frac{1}{2}(\Phi_{k,m}[n]+\|\mathbf{q}_m[n]-\mathbf{w}_k\|)^2-\lambda_{k,m}[n]\leq z_m[n], \quad (22)$$

where $\lambda_{k,m}[n]$ is defined in (25) in the proof.

Proof: The constraint (21b) is non-convex, for tractability, we change (21b) to an inequality constraint given by

$$\Phi_{k,m}[n] \leq \frac{z_m[n]}{\|\mathbf{q}_m[n]-\mathbf{w}_k\|}. \quad (23)$$

Since (23) is of the form "convex $\times$ convex $\leq$ linear", we use square of sum formula to make (23) a difference of convex function. Then, we get

$$\frac{1}{2}\left(\Phi_{k,m}[n]+\|\mathbf{q}_m[n]-\mathbf{w}_k\|\right)^2 - \frac{1}{2}\left(\Phi_{k,m}[n]^2+\|\mathbf{q}_m[n]-\mathbf{w}_k\|^2\right) \leq z_m[n]. \quad (24)$$

It can be observed that the (24) is of the form $f-g$, where f and g are both convex. To make (24) a convex constraint, g must be affine. Thus, we use first-order Taylor series expansion at any feasible point [9]. Then, g can be approximated as

$$\lambda_{k,m}[n]=\frac{1}{2}\left(\Phi^r_{k,m}[n]^2+\|\mathbf{q}^r_m[n]-\mathbf{w}_k\|^2\right)+\left(\Phi_{k,m}[n]-\Phi^r_{k,m}[n]\right) .\Phi^r_{k,m}[n]+\|\mathbf{q}^r_m[n]-\mathbf{w}_k\|(\|\mathbf{q}_m[n]-\mathbf{w}_k\|-\|\mathbf{q}^r_m[n]-\mathbf{w}_k\|), \quad (25)$$

where $\Phi^r_{k,m}[n], \mathbf{q}^r_m[n]$ is the value of $\Phi_{k,m}[n], \mathbf{q}_m[n]$ in the $r^{th}-$iteration, respectively. Using (25) in (24), we can obtain the convex constraint given in (22). ∎

Lemma 2: The constraint (19) can be replaced by its convex form which is given by

$$\frac{1}{2}\left(\alpha_{k,m}[n]+\|\mathbf{q}_m[n]-\mathbf{w}_k\|^2+z_m[n]^2\right)-\gamma_{k,m}[n]\leq\beta_{k,m}[n], \quad (26)$$

Algorithm 1 Algorithm to obtain the multi-UAVs trajectory

Input: $\mathbf{X}_I$, $\mathbf{X}_F$ H, $\mathbf{w}_k, \forall k \in \mathcal{K}$, $V^m_{max}, \forall m$.
Output: $\mathbf{T}=\{\mathbf{X}_m[n], \forall m, n\}$.

```
Initialize User association A^0 and power allocation P^0.
for n = 1 : N do
    Set S_D^1 = ||X_1[n] − X_I|| and S_D^2 = ||X_2[n] − X_F||.
    Set S_F^m = τ V_max^m (N − n), ∀m ∈ {1, 2}.
    if S_F^1 > S_D^1 and S_F^2 > S_D^2 then
        Solve P3.2 to obtain X_1[n], X_2[n].
    else if S_F^1 ≤ S_D^1 and S_F^2 > S_D^2 then
        Force U_1 to move in straight line towards X_I with
        velocity V_max^1 to obtain X_1[n].
        For fixed X_1[n], solve P3.2 to obtain X_2[n].
    else if S_F^1 > S_D^1 and S_F^2 ≤ S_D^2 then
        Force U_2 to move in straight line towards X_F with
        velocity V_max^2 to obtain X_2[n].
        For fixed X_2[n], solve P3.2 to obtain X_1[n].
    else
        Force U_1 and U_2 to move in straight line towards X_I
        and X_F with velocity V_max^1 and V_max^2, respectively,
        to reach the final location.
```

where $\gamma_{k,m}[n] = (\alpha^r_{k,m}[n]^2+(\|\mathbf{q}^r_m[n]-\mathbf{w}_k\|^2+z^r_m[n]^2)^2)(\alpha_{k,m}[n]-\alpha^r_{k,m}[n]\|\mathbf{q}^r_m[n]-\mathbf{w}_k\|)\alpha^r_{k,m}[n]+2((\|\mathbf{q}_m[n]-\mathbf{w}_k\|-\|\mathbf{q}^r_m[n]-\mathbf{w}_k\|)(\|\mathbf{q}^r_m[n]-\mathbf{w}_k\|^2+z^r_m[n]^2))+2(z_m[n]-z^r_m[n])z^r_m[n](\|\mathbf{q}^r_m[n]-\mathbf{w}_k\|^2+z^r_m[n]^2)$.

Proof: The proof is similar to Lemma 1, first using square of sum formula and then using using first-order Taylor series to make the second term affine, we can easily obtain (26) ∎

In the similar fashion, we can transform (17) to obtain

$$1+C\exp\left(-D\left[\tan^{-1}\Delta_{k,m}[n]-C\right]\right)- \left(\frac{1}{y^r_{k,m}[n]}+\frac{(y_{k,m}[n]-y^r_{k,m}[n])}{y^r_{k,m}[n]^2}\right)\leq 0. \quad (27)$$

To deal with the non-convex constraint in (9c), we introduce an auxiliary variable $D_{m,j}[n] = \{\mathbf{q}_m[n]-\mathbf{q}_j[n], \forall n, j \neq m\}$. Then, (9c) can be written as $\|D_{m,j}[n]\|^2 \geq D^2_{min}, \forall n, j \neq m$, so the left side $\|D_{m,j}[n]\|^2$ is convex in $D_{m,j}[n]$, then using first order Taylor expansion to obtain the global lower bound of convex function, we get

$$\|D_{m,j}[n]\|^2 \geq 2\left(D^r_{m,j}[n]\right)^T\left(D_{m,j}[n]-D^r_{m,j}[n]\right)+\|D^r_{m,j}[n]\|^2, \quad (28)$$

for a given $D^r_{m,j}[n]$. Using (9c), (28) is converted into

$$\xi^r_{m,j}[n]=2\left(\mathbf{q}^r_m[n]-\mathbf{q}^r_j[n]\right)^T\left(\mathbf{q}_m[n]-\mathbf{q}_j[n] -\mathbf{q}^r_m[n]-\mathbf{q}^r_j[n]\right)+\|\mathbf{q}^r_m[n]-\mathbf{q}^r_j[n]\|^2 \geq D^2_{min}. \quad (29)$$

Then, using the constraints (29), (27), (26), (22) and in place of (9c), (17), (19), (21b), respectively in **P3.2**, we obtain a convex optimization problem.

Note that finding the optimal location in each time slot does not guarantee that the UAV reaches their respective final location. Therefore, the idea behind obtaining the multi-UAVs trajectory is to compute the multi-UAV location using **P3.2** in a time slot for all n until $S^m_F > S^m_D$. Here, S^m_F denotes the distance that m^{th}-UAV can travel in the remaining $(N-n)$ time slots. S^m_D is the shortest distance between the present location of m^{th}-UAV and its final location. Thus, when $S^m_F \leq S^m_D, \forall m$, the m^{th}-UAV is forced to travel in a straight line towards its final location

Algorithm 2 Overall algorithm to obtain solution of (P1)

Input: $\mathbf{X}_I$, $\mathbf{X}_F$ H, $\mathbf{w}_k, \forall k \in \mathcal{K}$, $E^m_{max}, \forall m$, $V^m_{max}, \forall m$.

1: Initialize $\mathbf{A}^0$, $\mathbf{T}^0$, $\mathbf{P}^0$, set acceptable tolerance $\epsilon = 10^{-4}$, and iteration count $r = 0$, and $t = 0$. Set $V^{m,0}_{max} = V^m_{max}$.
2: **Repeat**
3: Fix $\{\mathbf{T}^r, \mathbf{P}^r\}$ and solve for $\mathbf{A}^{r+1}$ in problem **P2**.
4: Fix $\{\mathbf{A}^{r+1}, \mathbf{P}^r\}$, call Algorithm 1 to obtain $\mathbf{T}^{r+1}$ with $V^{m,t}_{max}$.
5: Fix $\{\mathbf{A}^{r+1}, \mathbf{T}^{r+1}\}$ and solve for $\mathbf{P}^{r+1}$ in problem **P4**.
6: Update $\{\mathbf{A}^r, \mathbf{T}^r, \mathbf{P}^r\}$ with $\{\mathbf{A}^{r+1}, \mathbf{T}^{r+1}, \mathbf{P}^{r+1}\}$, set $r = r + 1$, and calculate $\mathcal{R}^{r+1}$.
7: **Until** $\mathcal{R}^{r+1} - \mathcal{R}^r \leq \epsilon$.
8: Using $\mathbf{T}$, calculate $e^m_{tot} = \sum_{n=1}^{N} e_m[n], \forall m$. This $e_m[n]$ is computed using (5).
9: **Repeat**
10: Set $t = t + 1$.
11: Update $V^{m,t}_{max}$ using (31).
12: Repeat Steps 1-13.
13: **Until** $e^m_{tot} > E^m_{max}$.

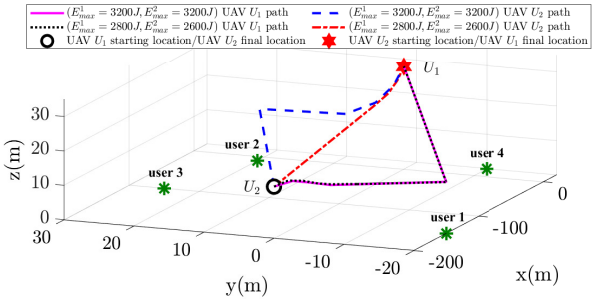

Fig. 2: Insights on UAV trajectories.

with V^m_{max} to reach the final location within the prescribed time. However, if one UAV is forced to travel in a straight line, the other UAV can still optimize its path using **P3.2**, only if $S^m_F > S^m_D$. Then, the overall algorithm to obtain the multi-UAVs trajectory is given in Algorithm 1.

C. UAV power allocation

For a given UAV trajectory and user association, the power allocation problem is given as

$$\mathbf{P4}: \quad \max_{\mathbf{P}} \quad \mathcal{R}, \quad s.t. \quad (4).$$

It can be observed that the problem **P4** comprises of concave objective function with linear inequality. Thus, problem **P4** is convex and can be efficiently solved via existing methods.

D. Overall Algorithm

Based on the above subproblems, here we present the overall algorithm to obtain the solution to **P1** based on AO. The steps to obtain the solution of **P1** are described in Algorithm 2. It first obtains the optimal **A**, **T**, and **P**, then using **T**, it computes the energy consumed by each UAV during its flight. If the manoeuvring energy is satisfied, then the obtained solution is the final solution. Otherwise, the maximum velocity by which the UAV now travels is updated and is given by

$$V^{m,t}_{max} = \frac{E^m_{max}}{e^m_{tot}} \times V^{m,t-1}_{max}, \tag{31}$$

where $V^{m,t-1}_{max}$ is the velocity of m^{th}-UAV at previous iteration. This update in velocity continues until the energy

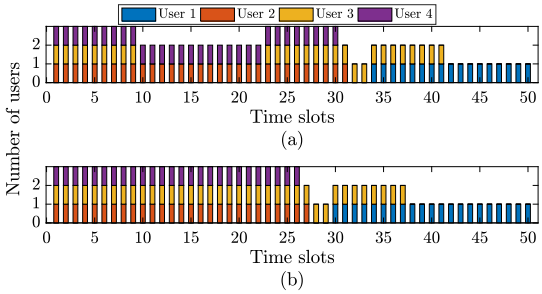

Fig. 3: Number and index of user associated with U_1.

constraint of the UAV is satisfied. Finally, the Algorithm 2 returns the solution to **P1**.

IV. Numerical Results

In this section, we validate the proposed scheme for multi-UAVs trajectory model. In our system, we consider $N = 4$ ground users over a given area [13]. The reference distance $\beta_0 = 1$ m and the environment parameters are set to $C = 10$, and D = 0.6. We consider the pathloss exponent and additional attenuation as $\bar{\alpha} = 2.3$, and $\kappa = 0.2$, respectively [14]. The minimum flying height H of the UAV is set to 15 m. The total flight time T is set to 20 s with $N = 50$ times slot. The UAV's starting location $\mathbf{X}_I$ = (-200,0,0) m, $\mathbf{X}_F$ = (0,0,30) m. The total communication power available with each UAV is $P_{max} = 0.1$ W [3], and the communication bandwidth B of the system is set to 20 MHz. The UAV's maximum velocity is $V^m_{max} = 30$ m/s. The parameters in energy consumption model are taken as follows: $P_o = 79.86$ W, $P_i = 88.63$ W, $v_o = 4.03$ m/s, $d_0 = 0.6$, $U_{tip} = 120$, $\rho = 1.225$ kg/m^3, $S = 0.05$, $s_{sp} = 0.0151$m^2, $W = 20$ N and $A = 0.503$ [10].

To get insights on the UAV trajectories, we plot Fig. 2 for two different cases of energy availability as follows: Case 1, $E^1_{max} = E^2_{max} = 3200$ J, and Case 2, $E^1_{max} = 2200$ J and $E^2_{max} = 2300$ J. These two cases are taken to analyze how the UAV trajectory is affected when less on-board energy is available with the UAV. Apart from this, Fig. 2 also shows the users location and the initial/final location of the UAV. For the same above cases, we also show the number and index of user that are associated to the existing UAV U_1 in Fig. 3(a), and 3(b), respectively.

It is observed from Fig. 2 that both the UAVs first travel towards the location at which the sum rate of the users (associated with that UAV) is maximum. This location is generally the user's location closest to the UAV, towards which the user's density is high. For example, as seen from Fig. 3(a), Initially users 2, 3, and 4 are associated with U_1. Out of which, users 2 and 3 are closer to each other, and user 2 is nearest to U_1. Therefore, U_1 travels towards user 2. On the other hand, only one user is associated with U_2; thus, it travels towards the associated user. The UAV follows the closest user because of the ability of the UAV to optimize the power allocated to each user. To maintain a maximum sum rate in each time slot, the UAV stays at that user's location and optimizes the power to achieve a maximal sum rate instead of following some other location. However, if UAV allocates equal power to each user, then, in that case, the UAV needs to compute the optimal location depending upon the users that are associated as seen in

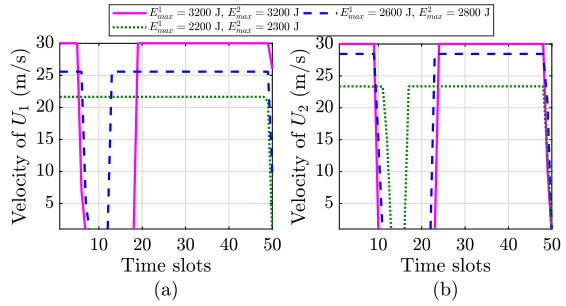

Fig. 4: Variation in (a) U_1 velocity, (b) U_2 velocity with E^m_{max}.

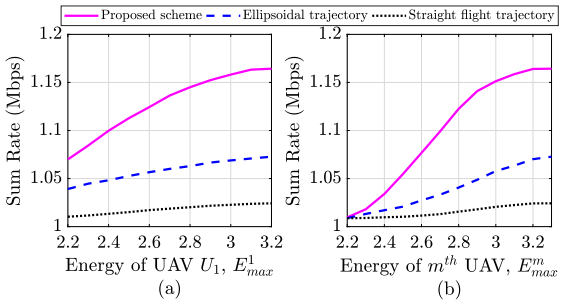

Fig. 5: Performance comparison of the proposed scheme.

[10] and then travel towards that optimal location. At later stages, the UAVs travel in a straight flight trajectory to reach their respective final locations to complete the replacement in a prescribed time. Thereafter, the user association and power allocation are optimized based on the straight flight trajectory taken by the UAV to reach the final location. Fig. 2 also shows that as we decrease the energy available with the UAV, the UAV now takes a shorter path to reach the final location. This is because the UAV energy model is a function of UAV velocity and to decrease the energy of the UAV's flight it decreases the UAV's velocity.

To show the variation in the UAV's velocity with the change in energy available with each UAV, we plot Fig. 4. It shows that the both UAVs initially fly at their maximum velocity and then decreases its velocity to hover at a location where the sum rate is maximum. Later, it again travels with the maximum velocity towards their final location to complete the replacement process in the predefined time. When energy is sufficiently small, the UAV travels with the same constant velocity to reach the final location. Thus, energy is compensated with the decrease in the UAV velocity.

To show the effectiveness of the proposed scheme, we plot Fig. 5 to compare the achievable sum rate with that of the straight flight trajectory and the ellipsoidal trajectory. Fig. 5(a) is plotted when $E^2_{max} = 3200$ J by varying E^1_{max} and Fig. 5(b) is plotted when E^m_{max} is varied assuming both the UAV's have same energy. It can be observed that the proposed scheme performs better than the existing trajectories. This is because, in straight flight and ellipsoidal trajectory, the UAV's takes a path irrespective of the users location, as a result, the pathloss increases and the UAV needs high communication power budget P_{max} to achieve a maximal achievable sum rate. Therefore, for a limited communication power budget, the proposed scheme provides 14% and 8% higher sum rate in comparison to the straight flight and ellipsoidal trajectory, respectively. Moreover, when the energy is very less, the sum rate of all the schemes will almost be same because the UAV will take a path that is closer to the straight line path. Furthermore, the sum rate also increases with the E^m_{max} because with E^m_{max}, the velocity by which the UAV can now travel increases and later, the sum rate becomes constant due to the presence of the velocity constraint of UAV.

V. Conclusion

In this paper, we design the UAV replacement framework in a UAV-assisted wireless communication system, where a fully charged UAV is launched to replace the existing UAV in such a way that achievable sum rate of the system is maximized. To do this, we jointly optimize the 3D UAV trajectories and resource allocation in the presence of the energy availability, velocity and collision avoidance constraints. The formulated problem is non-convex and an efficient iterative approach is proposed to solve the optimization problem. The numerical results are shown to get insights on the UAV trajectories. Furthermore, the effective of the proposed approach is shown in comparison to the benchmark scheme.

References

[1] Y. Zeng, R. Zhang, and T. J. Lim, "Wireless communications with unmanned aerial vehicles: Opportunities and challenges," *IEEE Commun. Mag.*, vol. 54, no. 5, pp. 36–42, May 2016.

[2] R. Singh, D. Saluja, and S. Kumar, "R-comm: A traffic based approach for joint vehicular radar-communication," *IEEE Trans. Intell. Veh.*, pp. 1–1, 2021.

[3] J. Ji, K. Zhu, D. Niyato, and R. Wang, "Joint cache placement, flight trajectory, and transmission power optimization for multi-UAV assisted wireless networks," *IEEE Trans. Wireless Commun.*, vol. 19, no. 8, pp. 5389–5403, Aug. 2020.

[4] Q. Wu, Y. Zeng, and R. Zhang, "Joint trajectory and communication design for multi-UAV enabled wireless networks," *IEEE Trans. Wireless Commun.*, vol. 17, no. 3, pp. 2109–2121, March 2018.

[5] J. Wang, Z. Na, and X. Liu, "Collaborative design of multi-UAV trajectory and resource scheduling for 6G-enabled internet of things," *IEEE Internet Things J.*, vol. 8, no. 20, pp. 15 096–15 106, Oct. 2021.

[6] Y. Wu, W. Fan, W. Yang, X. Sun, and X. Guan, "Robust trajectory and communication design for multi-UAV enabled wireless networks in the presence of jammers," *IEEE Access*, vol. 8, pp. 2893–2905, Dec. 2020.

[7] C. Shen, T.-H. Chang, J. Gong, Y. Zeng, and R. Zhang, "Multi-UAV interference coordination via joint trajectory and power control," *IEEE Trans. Signal Process.*, vol. 68, pp. 843–858, Jan. 2020.

[8] W. Zhang, Q. Wang, X. Liu, Y. Liu, and Y. Chen, "Three-dimension trajectory design for multi-UAV wireless network with deep reinforcement learning," *IEEE Trans. Veh. Technol.*, vol. 70, no. 1, pp. 600–612, Jan. 2021.

[9] W. Luo, Y. Shen, B. Yang, S. Wang, and X. Guan, "Joint 3D trajectory and resource optimization in multi-UAV-enabled IoT networks with wireless power transfer," *IEEE Internet Things J.*, vol. 8, no. 10, pp. 7833–7848, May 2021.

[10] N. Gupta, S. Agarwal, and D. Mishra, "Trajectory design for throughput maximization in UAV-assisted communication system," *IEEE Trans. Green Commun. Netw.*, vol. 5, no. 3, pp. 1319–1332, Sep. 2021.

[11] F. Zeng, Z. Hu, Z. Xiao, H. Jiang, S. Zhou, W. Liu, and D. Liu, "Resource allocation and trajectory optimization for QoE provisioning in energy-efficient UAV-enabled wireless networks," *IEEE Trans. Veh. Technol.*, vol. 69, no. 7, pp. 7634–7647, July 2020.

[12] A. Girdher, A. Bansal, and A. Dubey, "On the performance of SLIPT-enabled DF relay-aided hybrid OW/RF network," *IEEE Systems Journal*, pp. 1–12, 2022. doi.: 10.1109/JSYST.2021.3135957

[13] C. You, X. Peng, and R. Zhang, "3d trajectory design for UAV-enabled data harvesting in probabilistic LoS channel," in *Proc. IEEE Global Commun. Conf. (GLOBECOM)*, Dec. 2019, pp. 1–6.

[14] Y. Zeng, J. Xu, and R. Zhang, "Energy minimization for wireless communication with rotary-wing UAV," *IEEE Trans. Wireless Commun.*, vol. 18, no. 4, pp. 2329–2345, Apr. 2019.